

## Off-equilibrium magnetic properties in a model of repulsive particles for vortices in superconductors

This article has been downloaded from IOPscience. Please scroll down to see the full text article.

2001 J. Phys. A: Math. Gen. 34 L11

(<http://iopscience.iop.org/0305-4470/34/3/101>)

View [the table of contents for this issue](#), or go to the [journal homepage](#) for more

Download details:

IP Address: 171.66.16.97

The article was downloaded on 02/06/2010 at 09:09

Please note that [terms and conditions apply](#).

## LETTER TO THE EDITOR

## Off-equilibrium magnetic properties in a model of repulsive particles for vortices in superconductors

Mario Nicodemi and Henrik Jeldtoft Jensen

Department of Mathematics, Imperial College, 180 Queen's Gate, London SW7 2BZ, UK

Received 5 July 2000

### Abstract

We study the properties of a simple lattice model of repulsive particles diffusing in a pinning landscape. The behaviour of the model is very similar to the observed physics of vortices in superconductors. We compare and discuss the equilibrium phase diagram, creep dynamics, Bean critical state profiles, hysteresis of magnetization loops (including the second peak feature) and, in particular, 'ageing' in relaxations.

PACS numbers: 7510, 7425H

Important dynamical phenomena ranging from slow relaxations or hysteresis, to the anomalous 'second peak' in magnetization loops, are found in vortex physics of many different superconductors within a broad range of material parameters. This observation suggests that some basic general mechanisms are responsible for the observed phenomenology [1–4] and that schematic models from statistical mechanics can be successfully used to describe vortex matter [1–7].

We consider here a simple statistical mechanics model that appears to reproduce a very wide range of properties of vortices, ranging from dynamical behaviours to phase transitions. The model is an extension of a multiple-occupancy cellular-automaton-like model recently introduced by Bassler and Paczuski (BP) [7] to study vortex dynamics at the coarse-grained level. We introduce the vortex Hamiltonian in order to be able to consider non-zero-temperature effects in a consistent way and study them by Monte Carlo (MC) and replica theory methods. Our extension of the BP model also limits the occupancy of the individual lattice sites to correctly take into account the finiteness of the upper critical field. This point is of crucial importance for the phenomenological predictions of the model. This leads us to a restricted occupancy model (ROM).

We find that even the two-dimensional version of the model is able to qualitatively reproduce many features similar to those observed in real superconducting samples, including a reentrant equilibrium phase diagram, creep dynamics, hysteresis of magnetization loops, 'second peak' and others. Here, in particular, we describe its off-equilibrium magnetic properties. The model, simple and thus tractable, nevertheless appears to capture significant aspects of the essential physics and helps to establish a simple unified reference frame.

*The model.* A detailed description of the interaction potential,  $U(\vec{r})$ , between vortices depends on the considered region in the temperature–magnetic field ( $T$ – $H$ ) plane. For instance, at low field the London approximation can be used to derive two-body potentials [2], whereas at elevated fields other approximations, such as the lowest Landau level approximation, may become relevant (see e.g. [8]). As in the BP model, we consider here a coarse-grained lattice version of an interacting vortex system, with a coarse-graining length scale,  $l_0$ , of the order of the natural screening length of the problem (typically, the magnetic penetration length  $\lambda$ ). After coarse graining, the original interaction potential,  $U$ , is reduced to an effective Hamiltonian coupling  $A$ . In this way a drastic reduction of degrees of freedom is accomplished and the resulting schematic effective model can be more easily dealt with. The price to pay is the loss of information on scales smaller than  $l_0$ . However, some general features of the system behaviour can survive at the level of the coarse-grained description. In the above perspective, we consider below only the essential properties of vortex interaction, i.e. a mutual repulsion amongst vortices together with a spatially inhomogeneous pinning interaction. The present description can, of course, be refined by reducing the value of  $l_0$ . We consider the Hamiltonian

$$\mathcal{H} = \frac{1}{2} \sum_{ij} n_i A_{ij} n_j - \frac{1}{2} \sum_i A_{ii} n_i - \sum_i A_i^p n_i. \quad (1)$$

In equation (1),  $n_i \in \{0, \dots, N_{c2}\}$  is an integer occupancy variable equal to the number of particles on site  $i$ . The parameter  $N_{c2}$  importantly bounds the particle density per site below a critical value and represents the upper critical field  $B_{c2}$  in type-II superconductors. Particles also have a ‘charge’  $s_i = \pm 1$  and neighbouring particles with opposite ‘charge’ annihilate. The first term in equation (1) represents the repulsion between the particles [2]. Since the coarse-graining length is taken to be of order  $\lambda$ , we choose a finite-range potential:  $A_{ii} = A_0$ ;  $A_{ij} = A_1$  if  $i$  and  $j$  are nearest neighbours;  $A_{ij} = 0$  for all other pairs of sites. The second term in equation (1) just normalizes the particle self-interaction energy. The third term corresponds to a random pinning potential, with a given distribution  $P(A^p)$ , acting on a fraction  $p$  of lattice sites (below we use  $p = 1/2$ ). For simplicity we choose a delta-distributed random pinning:  $P(A^p) = (1-p)\delta(A^p) + p\delta(A^p - A_0^p)$ . To control the overall system ‘charge density’ we can add a chemical potential term  $-\mu \sum_i S_i$  to the above Hamiltonian ( $S_i = s_i n_i$ ). The parameters entering the model can be qualitatively related to material parameters of superconductors. The inter-vortex coupling  $A_0$  sets the energy scale. The ratio  $\kappa^* = A_1/A_0$  can be related to the Ginzburg–Landau parameter<sup>1</sup>  $\kappa = \lambda/\xi$  and, in general, is expected to be an increasing function of  $\kappa$ . The last parameter  $A^p$  is a fraction of  $A_0$ .

To understand the equilibrium properties of the ROM we briefly consider its replica mean-field (MF) theory. In this approximation the equilibrium phase diagram in the plane ( $H^*$ ,  $T^*$ ) (where  $T^* = k_B T/A_1$  and  $H^* = \mu/k_B T$ ) can be analytically dealt with (see figure 1). In absence of disorder it clearly shows a reentrant phase transition from a high-temperature low-density fluid phase to an ordered phase, in analogy to predictions in superconductors [1, 5].

For moderate values of the pinning energy ( $A_0^p \leq A_1$ ), a second-order transition still takes place, which at sufficiently strong pinning is expected to become a ‘glassy’ transition, as is seen in random-field Ising models [9]. For the two-dimensional lattice we consider below (in the limit  $A^p \rightarrow 0$ ), a numerical investigation is consistent with a first-order transition. In MF theory, the extension of the low- $T$  phase shrinks by increasing  $A_0^p$  (i.e. the highest critical temperature,  $T_m^*$ , decreases) and the higher is  $\kappa^*$  the smaller is the reentrant region. These findings are in agreement with experimental results on vortex phase diagrams (see [1] or, for instance, 2H-NbSe<sub>2</sub> superconductors from [10]).

<sup>1</sup> Asymptotically, the vortex line segment interaction is exponential,  $V(r) \sim V_0 \exp(-r/\sqrt{2}\lambda)$  [2]. One can write  $A_0/A_1 \propto V(0)/V(\text{const} \times \xi) \implies 1/\kappa^* \propto \exp(\text{const}/\kappa)$ .

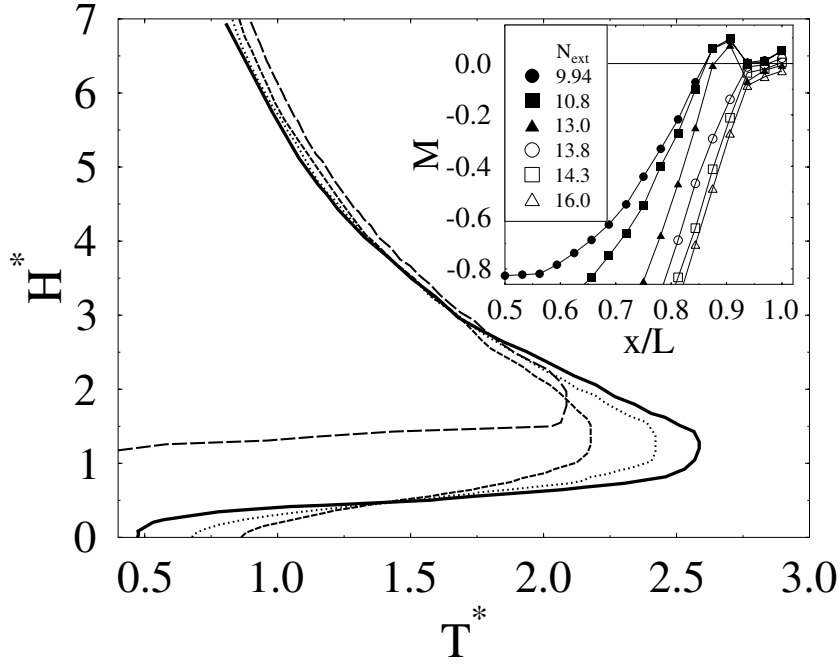


**Figure 1.** Main frame: the MF phase diagram of the ROM in the small-pinning-strength regime ( $A_0^p < A_0$ ), in the plane  $(H^*, T^*)$  (here  $H^* = \mu/k_B T$ ,  $T^* = T/A_1$  are the dimensionless chemical potential and temperature), for  $\kappa^* = 10$  and  $A_0^p = 0.0; 0.5; 0.75$  (respectively full, dotted and dashed curves) and  $\kappa^* = 3.3$  and  $A_0^p = 0.0$  (long-dashed curve). Inset: the magnetization profile,  $M(x)$ , as a function of the transversal spatial coordinate  $x/L$  ( $L$  is the system linear size), recorded while ramping the external field,  $N_{\text{ext}}$  (for the shown values), in the two-dimensional ROM ( $\kappa^* = 0.26$ ,  $T = 0.3$ ,  $\gamma = 1.1 \times 10^{-3}$ ). Notice the change in shapes for  $N_{\text{ext}}$  smaller or larger than  $N_p \simeq 13.5$  (filled versus empty symbols).

We now go beyond MF theory and discuss the dynamical behaviour of the model. We performed MC simulations on a two-dimensional square lattice system (we use typically  $L^2 = 32^2$ ) described by equation (1). The system is periodic in the  $y$ -direction and has the two opposite edges in the  $y$ -direction in contact with a reservoir of particles. The reservoir is described by  $\mathcal{H}$  with  $A_i^p = 0 \forall i$  and kept at a given density  $N_{\text{ext}}$ . Particles undergo diffusive dynamics and are introduced and escape the system only through the reservoir. The parameters of our simulations are usually  $A_0 = 1.0$ ;  $A_0^p = 0.3$ ;  $N_{c2} = 27$ . We have sampled several values of  $\kappa^* \in [0, 0.3]$ .

We are interested in the dynamical properties of the system in the low- $T^*$  region of the above phase diagram. Here the two-dimensional model has interesting magnetic hysteretic behaviours. In our MC simulations we ramp  $N_{\text{ext}}$  (starting from zero and later back to zero) at a given rate  $\gamma = \Delta N_0/\tau$  and record the magnetization,  $M = N_{\text{in}} - N_{\text{ext}}$  ( $N_{\text{in}} = \langle \sum_i s_i n_i \rangle / L^d$  is the ‘charge’ density inside the system) as a function of  $N_{\text{ext}}$ . Such a ramping induces a Bean-like profile in our lattice (inset of figure 1) with a structure similar to some experimental data (see, for instance, [11]).

At low temperatures<sup>2</sup> ( $T \leq 5$ ), a pronounced hysteretic magnetization loop is seen (see figure 2), and when  $\kappa^*$  is high enough ( $\kappa^* \geq 0.25$ ) a definite second peak appears in  $M$ . In the present case the origin of the second peak is very simple. At high density and  $\kappa^*$ , groups

<sup>2</sup> We use  $A_0 = 1.0$  as the energy unit and set  $k_B = 1$ .

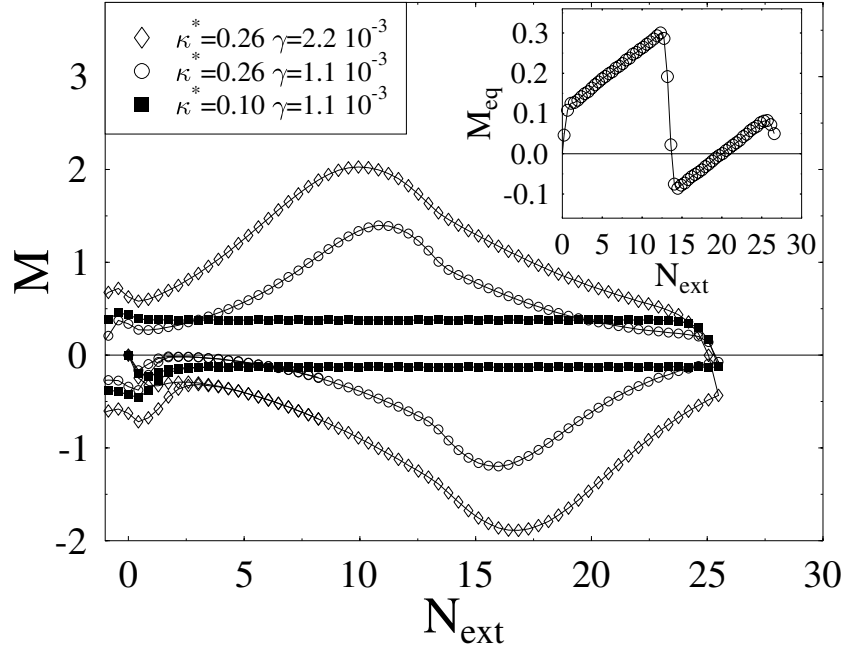


**Figure 2.** Main frame: the magnetization,  $M$ , as a function of the applied field density,  $N_{\text{ext}}$ , in the two-dimensional ROM for  $\kappa^* = 0.1, 0.26$  at  $T = 0.3$  and the shown sweep rates  $\gamma$ . The locations of the peak, different in the increasing and decreasing branches, depend on  $\gamma$  and approach the same value in the limit  $\gamma \rightarrow 0$ . Inset: the equilibrium value of  $M$  (i.e. when  $\gamma \rightarrow 0$ ) for  $\kappa^* = 0.26$  at  $T = 0.3$ .

of vortices, frustrated in minimizing their repulsive interaction energy, are forced to cluster together, forming macroscopically extended energetic barriers, which cage other diffusing vortices. In figure 3 we plot the average energy barrier,  $\Delta E(N_{\text{ext}})$ , that a particle meets during the same runs for  $M$  as shown in figure 2. A ‘trial’ vortex approaching groups of clustered vortices has to pass over these barriers to move further. This dynamically generates the second peak. The final decrease in  $M$  at high  $N_{\text{ext}}$  is, here, due to a ‘softening’ of these barriers caused by saturation effects related to the finite value of  $N_{c2}$ . The first peak in the magnetization stems from the fact that density variations in the reservoir are only slowly transmitted in the system when it is in the low-density ‘fluid’ phase. The second peak and hysteretic loops at moderate to high  $\kappa^*$  are also present when  $A_0^p \rightarrow 0$  ( $A_0^p$  also determines the difference in the amplitude of  $|M|$  between the increasing and decreasing ramps). Very similar magnetization data are observed in a number of different superconductors from intermediate to high  $\kappa$  values (see, for instance, [4, 10, 12]).

The actual shape of loops strongly depends on the parameters of the dynamics (and system size). In particular, the sweep rate of the external field,  $\gamma$ , is very important. As soon as the inverse sweep rate is smaller than the characteristic relaxation time (which can be extremely long, inaccessible on usual observation time scales, see below) strong off-equilibrium effects are present, such as metastability or ‘memory’ and ‘ageing’ [3, 10, 12]. As a first example of these facts, we show in the right inset of figure 3 the dependence of the second peak height,  $M_p$ , on  $\gamma$ . At low temperatures ( $T \leq 1$ ) and not too low  $\kappa^*$  ( $\kappa^* \geq 0.28$ ),  $M_p$  is approximately logarithmically dependent on  $\gamma$  over several decades:

$$M_p(\gamma) \simeq M_0 + \Delta M \ln(\gamma). \quad (2)$$

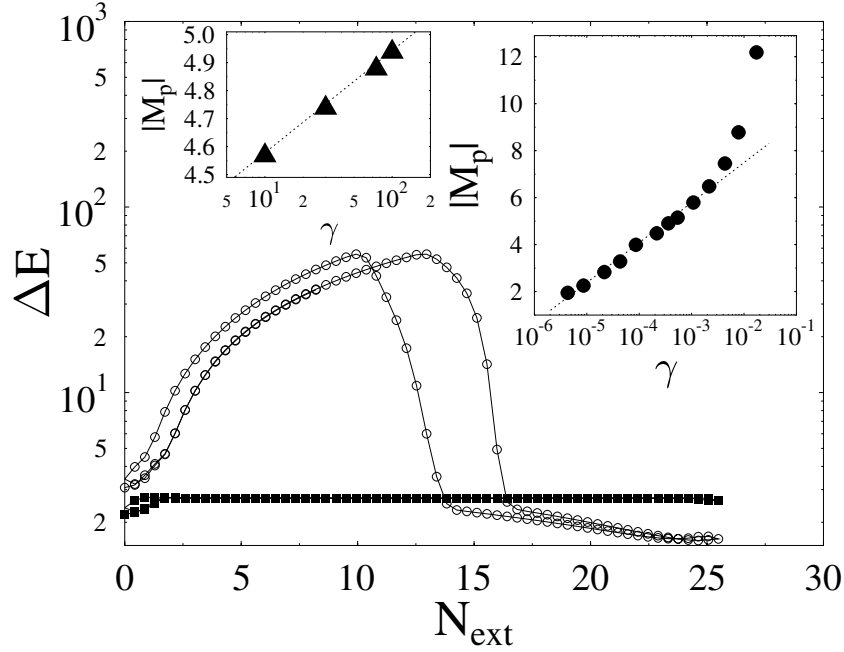


**Figure 3.** Main frame: the average energy barrier,  $\Delta E$ , that a particle meets during diffusion in the same ROM lattices as figure 2. Inset right: the second magnetization peak height in the ROM as a function of the sweep rate  $\gamma$  for  $\kappa^* = A_1/A_0 = 0.28$  at  $T = 0.3$ . Inset left: the second magnetization peak,  $M_p$  ( $\text{A m}^2 \times 10^3$ ), in a single crystal of  $\text{YBa}_2\text{Cu}_4\text{O}_8$  at temperature 20 K as a function of the sweep rate,  $\gamma$  ( $\text{mT s}^{-1}$ ) (from [13]).

Such a behaviour approaches a power law  $M_p \sim \gamma^x$  at lower  $\kappa^*$  (for instance,  $x \sim 1/2$  at  $\kappa^* = 0.26$ ). Eventually, when  $\gamma$  is smaller than a characteristic threshold,  $\gamma_t$ ,  $M_p$  exponentially saturates to its asymptotic value (this usually is orders of magnitude smaller than  $M_p(\gamma)$  at high  $\gamma$ ). Interestingly these findings are also very close to what is experimentally observed in superconductors [3,4]; an example from an  $\text{YBa}_2\text{Cu}_4\text{O}_8$  sample (from [13]) is given in the left inset of figure 3. The threshold,  $\gamma_t$ , is strongly dependent on the system density  $N_{\text{in}}$  (and system size) and is a rapidly decreasing function of  $\kappa^*$ ; for instance at  $T = 0.3$ , for  $N_{\text{ext}} = N_p$  ( $N_p$  is the location of  $M_p$ ),  $\gamma_t|_{\kappa^*=0.26} \simeq 4.5 \times 10^{-5}$  but  $\gamma_t|_{\kappa^*=0.28} \leq 10^{-6}$ .  $\gamma_t^{-1}(T, N_{\text{in}}; \kappa^*, L)$  is a measure of the system characteristic equilibration times (which can be huge).

Seemingly a dynamical phenomenon, in the ROM the second peak is related to a true transition: in the  $\gamma \rightarrow 0$  limit, its location,  $N_p$ , is associated with a sharp jump in  $M_{\text{eq}} \equiv \lim_{\gamma \rightarrow 0} M(\gamma)$ , where its fluctuations increase with system size (see the inset of figure 2). These findings are consistent with experiments (for instance, see [10]) and to some extents reconcile opposite descriptions (‘static’ versus ‘dynamic’) of the phenomenon.

It is also interesting to consider the ‘creep rate’,  $Q = \frac{\partial \ln M}{\partial \ln \gamma}$ , which is often associated with a measure of the intrinsic energy barriers in the creep process [3]. Experimentally,  $Q$  is a non-trivial function of the magnetic field (see for instance [3, 13]). We find that, due to the very long relaxation times,  $Q(N_{\text{ext}})$  is in itself a (slowly varying) function of  $\gamma$ , up to when  $\gamma$  is smaller than the smallest  $\gamma_t$ . In figure 4 we show how  $Q$  depends on  $\gamma$  in the ROM: for  $T = 0.3$  and  $\kappa^* = 0.28$  we plot as a function of  $N_{\text{ext}}$  the average of  $Q$  over two different  $\gamma$  intervals,  $\gamma \in [5 \times 10^{-3}, 10^{-1}]$  (filled circles) and  $\gamma \in [5 \times 10^{-4}, 5 \times 10^{-3}]$  (filled squares). The difference between the two is apparent. We note a remarkable correspondence

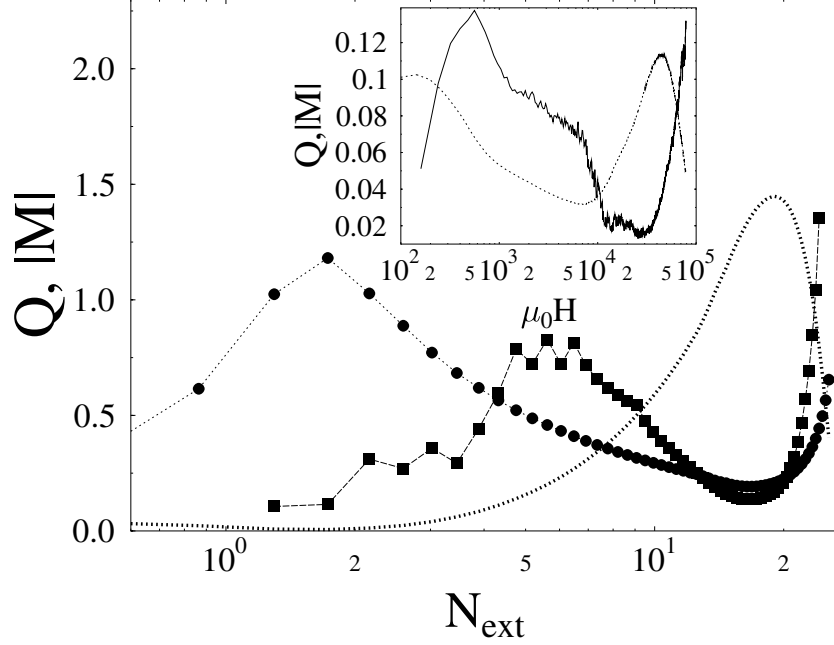


**Figure 4.** Main frame: for the same ROMs as the right inset of figure 3 with  $\kappa^* = 0.28$ , the ‘creep rate’  $Q \equiv \frac{\partial \ln M}{\partial \ln \gamma}$  averaged over the intervals  $\gamma \in [5 \times 10^{-3}, 10^{-1}]$  (filled circles) and  $\gamma \in [5 \times 10^{-4}, 5 \times 10^{-3}]$  (filled squares), is plotted as a function of  $N_{\text{ext}}$ . For comparison, a corresponding magnetization loop ( $M \rightarrow M/4$  to have a clear scale on the y-axis) is also shown (dotted curve). Inset: the creep rate (for  $\gamma \in [10, 100]$  mT s $^{-1}$ , full curve) and magnetization loop ( $4 \times 10^2$  A m $^2$ , dotted curve) as a function of the external magnetic field  $\mu_0 H$  (T) in the same YBa $_2$ Cu $_4$ O $_8$  sample as figure 3.

with experimental data for YBa $_2$ Cu $_4$ O $_8$ , shown for the quoted sample in the inset of figure 4.

The presence of the above ‘memory’ effects indicate that the system, on the observed time scales, can be well off equilibrium. To reveal the underlying non-stationarity of the dynamics we consider two time correlation functions and, at a given  $N_{\text{ext}}$ , we record<sup>3</sup> ( $t > t_w$ )

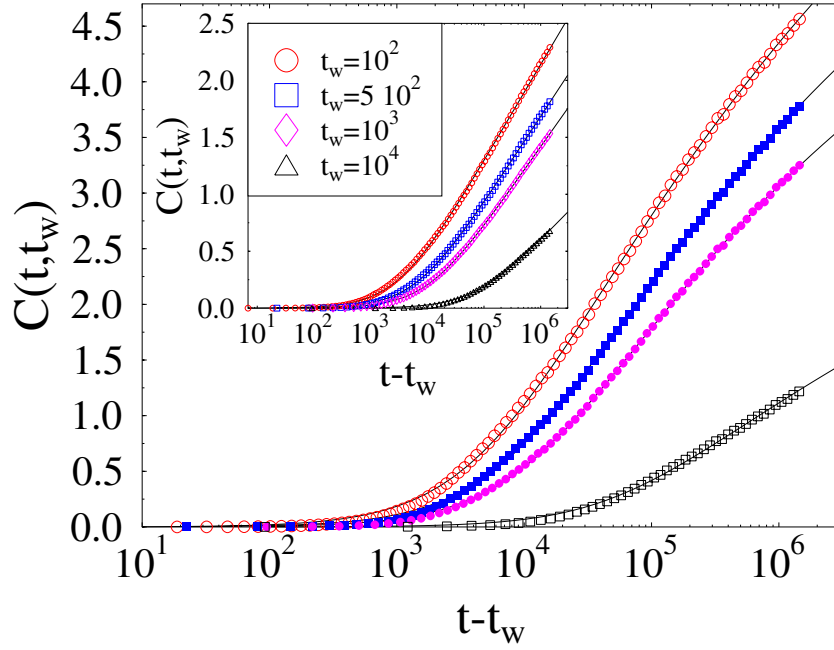
$$C(t, t_w) = \langle [N_{\text{in}}(t) - N_{\text{in}}(t_w)]^2 \rangle. \quad (3)$$

Figure 5 clearly shows that  $C(t, t_w)$  exhibits strong ‘ageing’: it explicitly depends on both times, in contrast to situations close to equilibrium, where  $C$  is a function of the time difference  $t - t_w$ . In particular at high  $\kappa^*$  and low  $T$  (where relaxation times are very high)  $C(t, t_w)$  can be well fitted by a generalization of a known interpolation formula, often experimentally used [1], which now depends on the *waiting time*,  $t_w$ :

$$C(t, t_w) \simeq C_\infty \left\{ 1 - \left[ 1 + \frac{\mu T}{U_c} \ln \left( \frac{t + t_0}{t_w + t_0} \right) \right]^{-1/\mu} \right\}. \quad (4)$$

We found that to take  $\mu \simeq 1$  is consistent with our data. Notice the presence of *scaling properties*: for not too short times  $C$  is a function of only the ratio  $t/t_w$ :  $C(t, t_w) \sim \mathcal{S}(t/t_w)$ . This is a fact in agreement with general scaling in off-equilibrium dynamics (see [15]) and in strong analogy with other systems (from glass formers to granular media [14–17]). Experimental measurements of  $C(t, t_w)$  would be *very* valuable.

<sup>3</sup> Time is measured in units of an MC full lattice sweep.



**Figure 5.** Time relaxation of the two-time vortex-density correlation function,  $C(t, t_w)$ , in the two-dimensional ROM, recorded at  $T = 0.1$  ( $\kappa^* = 0.28$ ) for the shown  $t_w$  at  $N_{\text{ext}} = 4, 16$  (respectively inset and main frame). Continuous curves are logarithmic fits.

(This figure is in colour only in the electronic version, see [www.iop.org](http://www.iop.org))

In conclusion, in the context of a simple tractable model we have depicted a panorama of magnetic properties of vortices in type-II superconductors. Even the two-dimensional version of the model has many interesting features in correspondence with experimental results and allows clear predictions on the nature of vortex dynamics. The origin of the slow off-equilibrium relaxation (observed at low  $T$ ) is caused by the presence of very high free energy barriers *self-generated* by the strong repulsive interaction between particles at high densities (for  $\kappa^*$  above a threshold). In this respect the pinning potential plays a minor role. For instance, the presence of a ‘second peak’ in  $M$  is also observed in the limit  $A^p \rightarrow 0$ . The second peak does not mark the transition to a ‘glassy’ phase, but is also present in such a case.  $A^p$  sets the position and amplitude of the reentrant order–disorder transition line, which is in turn distinct from the second-peak locations.

At low temperatures on typical observation timescales, the system is strongly off equilibrium. This is most clearly seen from ‘ageing’ found in two-time correlation functions. These obey scaling properties of purely dynamical origin. An experimental check of these results would be extremely important to elucidate the true nature of vortex dynamics.

We thank L Cohen and G Perkins for useful discussions and for the  $\text{YBa}_2\text{Cu}_4\text{O}_8$  data. This work was supported by the EPSRC and PRA-INFM-99.

## References

- [1] Blatter G, Feigel'man M V, Geshkenbein V B, Larkin A I and Vinokur V M 1994 *Rev. Mod. Phys.* **66** 1125
- [2] Brandt E H 1995 *Rep. Prog. Phys.* **58** 1465



- 
- [3] Yeshurun Y, Malozemoff A P and Shaulov A 1996 *Rev. Mod. Phys.* **68** 911
  - [4] Cohen L F and Jensen H J 1997 *Rep. Prog. Phys.* **60** 1581–672
  - [5] Nelson D R 1988 *Phys. Rev. Lett.* **60** 1973
  - [6] Fisher M P A 1989 *Phys. Rev. Lett.* **62** 1415  
Gianmarchi A and Le Doussal P 1994 *Phys. Rev. Lett.* **72** 1530  
Gurevich A and Vinokur V M 1999 *Phys. Rev. Lett.* **83** 3037
  - [7] Bassler K E and Paczuski M 1998 *Phys. Rev. Lett.* **81** 3761  
Bassler K E, Paczuski M and Reiter G F 1999 *Phys. Rev. Lett.* **83** 3956
  - [8] Kienappel A K and Moore M A 1999 *Phys. Rev. B* **60** 6795
  - [9] Nattermann T 1998 *Spin Glasses and Random Fields* ed P Young (Singapore: World Scientific)
  - [10] Ghosh K *et al* 1996 *Phys. Rev. Lett.* **76** 4600  
Banerjee S S *et al* 1999 *Preprint cond-mat/9911324*
  - [11] Giller D *et al* 1997 *Phys. Rev. Lett.* **79** 2542
  - [12] Paltiel Y *et al* 2000 *Nature* **403** 398
  - [13] Cohen L F *et al* 1994 *Physica C* **230** 1  
Perkins G K *et al* 1995 *Phys. Rev. B* **51** 8513  
Totty J *PhD Thesis*
  - [14] Bouchaud J P, Cugliandolo L F, Kurchan J and Mezard M 1998 *Spin Glasses and Random Fields* ed P Young (Singapore: World Scientific)
  - [15] Coniglio A and Nicodemi M 1999 *Phys. Rev. E* **59** 2812
  - [16] Angell C A 1995 *Science* **267** 1924
  - [17] Nicodemi M and Coniglio A 1999 *Phys. Rev. Lett.* **82** 961